A Study of Electrochemically grown Prussian Blue Films using Fourier-transform Infra-red Spectroscopy

Paul A. Christensen, Andrew Hamnett,* and Simon J. Higgins
Department of Chemistry, The University, Newcastle-Upon-Tyne NE1 7RU

The electrochemical cycling of films of Prussian Blue (PB), deposited by electroreduction onto Pt, have been studied by *in situ* Fourier-transform i.r. spectroscopy under potential control. The results are compared with those obtained earlier using ellipsometry. The behaviour of the films can be understood in terms of a two-phase model, in agreement with the ellipsometric results. The outer, porous film, present in variable amount, is found to be largely 'insoluble' PB whereas the inner film, which constitutes the majority of material present in the experiments, changes to 'soluble' PB on repeated reductive cycling. The two phases have quite different i.r. spectra, and their relative intensities change as a function of cycling, in agreement with earlier work. The process of oxidation to Prussian Yellow reveals the kinetic sluggishness of the outer layer particularly clearly.
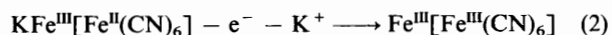
The history of Prussian Blue (PB) as an identifiable dye extends back nearly 300 years, and it is still the subject of a considerable research effort,[1] largely as a result of the discovery that films of PB could be grown electrochemically and that potential cycling of these films led to electrochromic effects.[2] The growth of Prussian Blue films on a variety of substrates can be achieved electrochemically by reduction of a solution containing both iron(III) and hexacyanoferrate(III) ions. If the resultant modified electrode is transferred to aqueous KCl, potential cycling leads both to *reduced* (Prussian White, PW) and *oxidised* (Prussian Yellow, PY) forms.[3] In addition to the obvious electrochromic applications of such films,[4] they also have potential applications as electrocatalysts for fuel cells, redox matrices for sensors, and as electrodes for batteries.[5]

Prussian Blue exists in two forms, the so-called 'insoluble' $Fe^{III}_4[Fe^{II}(CN)_6]_3$ and the 'soluble' $KFe^{III}[Fe^{II}(CN)_6]$; the terms refer to ease of peptisation rather than solubility. Keggin and Miles[6] suggested a face-centred cubic lattice for soluble PB with the high-spin iron(III) and low-spin iron(II) ions co-ordinated octahedrally by –NC and –CN ligands respectively. It was assumed that K^+ ions occupied interstitial sites. An X-ray crystallographic study of crystals of insoluble PB, grown extremely slowly under carefully controlled conditions in the absence of K^+ ions, showed a primitive cubic lattice, with a quarter of the $Fe(CN)_6$ sites vacant.[7] The vacant N positions are occupied by water molecules which complete the octahedral co-ordination about Fe^{III}.

To date, uncertainty about which formulation is appropriate for the electrochemically deposited material has dogged electrochemical studies. Detailed mechanisms for film growth and potential cycling are not well understood, with the result that optimisation of devices based upon PB has proved difficult. Initially, it was presumed that because the films were grown from media containing K^+ they consisted of soluble PB.[8] Thus, reduction to PW could be represented by equation (1) and
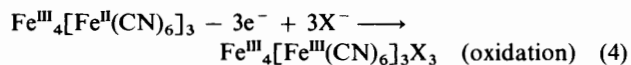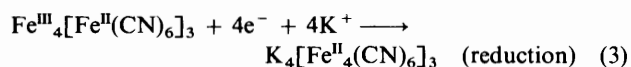
$$KFe^{III}[Fe^{II}(CN)_6] + e^- + K^+ \longrightarrow K_2Fe^{II}[Fe^{II}(CN)_6] \quad (1)$$
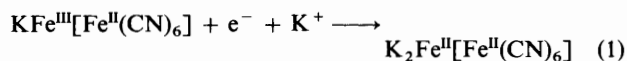
oxidation to PY by equation (2). Later, Itaya and co-workers[9]

$$KFe^{III}[Fe^{II}(CN)_6] - e^- - K^+ \longrightarrow Fe^{III}[Fe^{III}(CN)_6] \quad (2)$$

proposed that the film always consists of insoluble PB, on the basis of X-ray photoelectron and Auger spectroscopy of freshly

deposited films which showed no K^+ to be present, and the ratio of the charge passed on oxidation to that passed on reduction, which was 0.72 rather than 1.00, *i.e.* equations (3) and (4) are applicable.

$$Fe^{III}_4[Fe^{II}(CN)_6]_3 + 4e^- + 4K^+ \longrightarrow K_4[Fe^{II}_4(CN)_6]_3 \quad (reduction) \quad (3)$$

$$Fe^{III}_4[Fe^{II}(CN)_6]_3 - 3e^- + 3X^- \longrightarrow Fe^{III}_4[Fe^{III}(CN)_6]_3X_3 \quad (oxidation) \quad (4)$$

Other workers, employing *in situ* spectroelectrochemical[7b] and quartz-crystal microbalance[10] techniques, showed that the films were deposited as insoluble PB even in the presence of K^+, but on potential cycling to PW a remarkable transformation to the soluble form occurs. Initially, it was thought that this transformation was quantitative, but more recent data have indicated that complete conversion into the soluble form may not occur, and that even the well cycled film may contain both forms.[11]

We have been interested in using *in situ* ellipsometry and Fourier-transform infrared (F.t.i.r.) spectroscopy to probe modified electrodes under potential control.[12] We have used ellipsometry to study films of PB, and concluded that, as formed, the film was biphasic, with an inner relatively compact layer that underwent complete conversion on cycling into PW and an outer more porous layer whose conversion kinetics, particularly during oxidation, were significantly more sluggish.[13]

The disadvantage of ellipsometry as a probe lies primarily in the difficulty of relating the observed refractive indices to the molecular structure of film. In order to probe the latter, a molecular spectroscopic technique must be used, and the recent development of *in situ* subtractively normalised F.t.i.r. offers, in principle, a most powerful probe of the Prussian Blue film structure.[14,15] In this study, subtractively normalised F.t.i.r. was applied to the Prussian Blue films, and some conclusions about the detailed structure of the film are presented.

Experimental

The compounds KCl, KH_2PO_4, NaOH, HCl, $FeCl_3$, and $K_3[Fe(CN)_6]$ (BDH AnalaR) were used as received. Water was doubly distilled and pyrolysed in a stream of oxygen at 1100 °C. The subtractively normalised F.t.i.r. cell was a standard
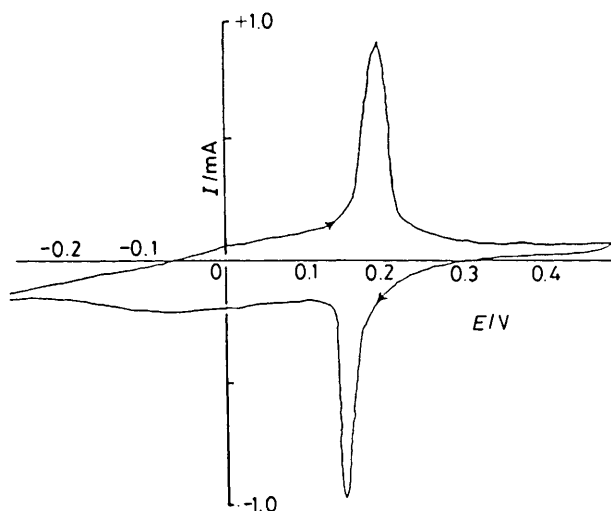
Figure 1. Cyclic voltammogram of a Prussian Blue film grown for 30 s at 0.5 V in 0.01 mol dm^{-3} HCl–0.1 mol dm^{-3} KCl on Pt and cycled in pH 6 buffer solution. The voltammogram was collected after 20 cycles between -0.2 and $+0.5$ V in 0.5 mol dm^{-3} KCl, with the electrode pulled back from the cell window, at 5 mV s^{-1}

three-electrode cell employing a calcium fluoride window and a standard thin-layer configuration. Details of the latter, along with the methods employed, are given elsewhere.[16] The electrodes were platinum or edge-carbon discs, 7 mm in diameter and 3 mm thick, sheathed in epoxy resin. Potentials are quoted vs. saturated calomel electrode (s.c.e.). The electrodes were polished with aqueous suspensions of 0.3-, 0.075-, and 0.015-µm alumina, followed by sonication in water for 20 min. The Prussian Blue films were grown as follows: a solution containing 5 mmol dm^{-3} FeCl$_3$, 5 mmol dm^{-3} K$_3$[Fe(CN)$_6$], 0.1 mol dm^{-3} KCl, and HCl to pH 1—2 was purged with N$_2$ for 20 min prior to admission into the cell. The electrode was pulled back from the window and held initially at $+0.9$ V. The potential was then stepped down to $+0.5$ V for 30—90 s and finally switched to open circuit, or maintained at $+0.5$ V whilst fresh nitrogen-purged KCl solution was admitted to the cell. Experiments referred to as conducted in pH 6 buffer employed a solution 0.05 mol dm^{-3} in KH$_2$PO$_4$ and 0.1 mol dm^{-3} in KCl, adjusted to pH 6 by the addition of NaOH.

The spectrometer was purged, and the air bearing driven by dry N$_2$ from a cryogenic boil-off. The nitrogen feed was also used to purge solutions and drive the in situ delivery device,[16] which was connected to the inlet port of the cell by poly(vinyl chloride) (pvc) tubing. The outlet port of the cell was connected to a waste receptacle.

The F.t.i.r. spectrometer was a Digilab Qualimatic QS100 fitted with a wide-range mercury cadmium telluride detector and interfaced to a 68000-based micro-computer (Oxsys Micros). The latter contained and controlled the potentiostat card that provided the potential at the working electrode; it also controlled the spectrometer.

Spectra were collected a 8 cm^{-1} resolution. The single-step or staircase[14] spectra consisted of 69 scans (100 s) at each potential. The results are presented as $(S_n - S_1)/S_n$, where S_1 is the spectrum collected at the base potential E_1, and S_n is the spectrum collected at the potential E_n. The reflected intensity is represented as $(\Delta R/R)$, where no correction has been made for reflection from the outer surface of the window. In all of the spectra shown, features pointing up (to positive $\Delta R/R$) are due to loss of the absorbing species at the potential E_n; bands pointing down (to negative $\Delta R/R$) correspond to a gain of the chromophore at E_n.

Results and Discussion

(a) *Interconversion of Prussian Blue (PB) and Prussian White (PW) in well cycled Films.*—Figure 1 shows a cyclic voltammogram of a Prussian Blue film grown for 30 s as described above on platinum and cycled in 0.1 mol dm^{-3} KCl solution with the electrode pulled back from the window of the cell. The film was cycled 20 times between -0.2 and $+0.5$ V prior to the collection of the voltammogram, which in this case was obtained in pH 6 buffer at 5 mV s^{-1}. The potential of the platinum electrode was then held at -0.3 V and a reference spectrum collected prior to stepping the potential to successively higher values and collecting further scans during the conversion from PW into PB. These spectra were normalised to the reference spectrum and the results are presented in Figure 2(a) and (b) for the cyanide stretching region.

In order to interpret these difference spectra more easily, the single-beam (s.b.) spectra are presented in Figure 2(c). These spectra are *not* absolute, in that they are convoluted by source and detector response, but the intensities of the cyanide absorptions in the wavelength region corresponding to cyanide stretch are sufficiently high to be seen easily above the background.

From Figure 2 it can be seen that increasing the potential leads to gain features at approximately 2 100 and 2 050 cm^{-1} and a loss feature at approximately 2 080 cm^{-1}. Both the gain feature at 2 100 cm^{-1} and the loss feature at 2 080 cm^{-1} apparently show a potential-dependent shift, an initially puzzling observation, particularly because the potential dependence of the loss peak at 2 080 cm^{-1} must be an artifact: this loss is of features present only in the reference spectrum which is taken at a single potential. We can resolve this problem by examining the s.b. spectrum of Figure 2(c), which shows that, in the spectral region between 2 060 and 2 130 cm^{-1}, PW shows a relatively narrow band centred at 2 085 cm^{-1} with a half-width of approximately 20 cm^{-1}. As the potential is raised, this shows an initial slight shift and broadening. Then, on entering the potential region where the sharp main peak is found in the slow-scan cyclic voltammogram (Figure 1), the rapid growth of a second, much broader band, centred at 2 106 cm^{-1} is seen. At the intermediate potentials (ca. 0.15—0.3 V), bands at 2 106 and 2 085 cm^{-1} exist together and the differences in intensity and width between the two bands gives rise to a complex series of intensity changes in the difference spectra.

In addition to the changes in the main cyanide absorption region, there is the appearance of a shoulder at 2 050 cm^{-1}. The difference spectra show clearly that this shoulder appears at -0.2 V, grows to a maximum in intensity at $+0.15$ V, and then collapses at higher potentials, as shown in Figure 3. This behaviour is associated with the initial broadening of the main peak, but not with the peak at 2 106 cm^{-1}, and again corresponds to the rather irreversible structure seen in the anodic scan of the cyclic voltammogram, which appears at -0.2 V and extends to the start of the main wave near $+0.2$ V.

(b) *Interconversion of Prussian Blue and Prussian White in freshly grown Films.*—After formation of the film, the initial potential cycles are known to be atypical. As indicated above, it is believed that at least partial conversion into 'soluble' PB takes place, and to explore this process spectra were taken for the first reduction and reoxidation cycles. The corresponding s.b. spectra are shown in Figure 4, and these may be compared to those of Figure 2(c). The spectra of the initial 'insoluble' PB consists of a broad band in the CN stretching region centred near 2 075 cm^{-1}. On reduction, this sharpens appreciably to a band centred near 2 080 cm^{-1}, but the process is accompanied by the appearance of a transitory shoulder near 2 106 cm^{-1}. Reoxidation gives rise to a much stronger permanent feature at 2 106 cm^{-1} and the broad peak near 2 075 cm^{-1} reappears,
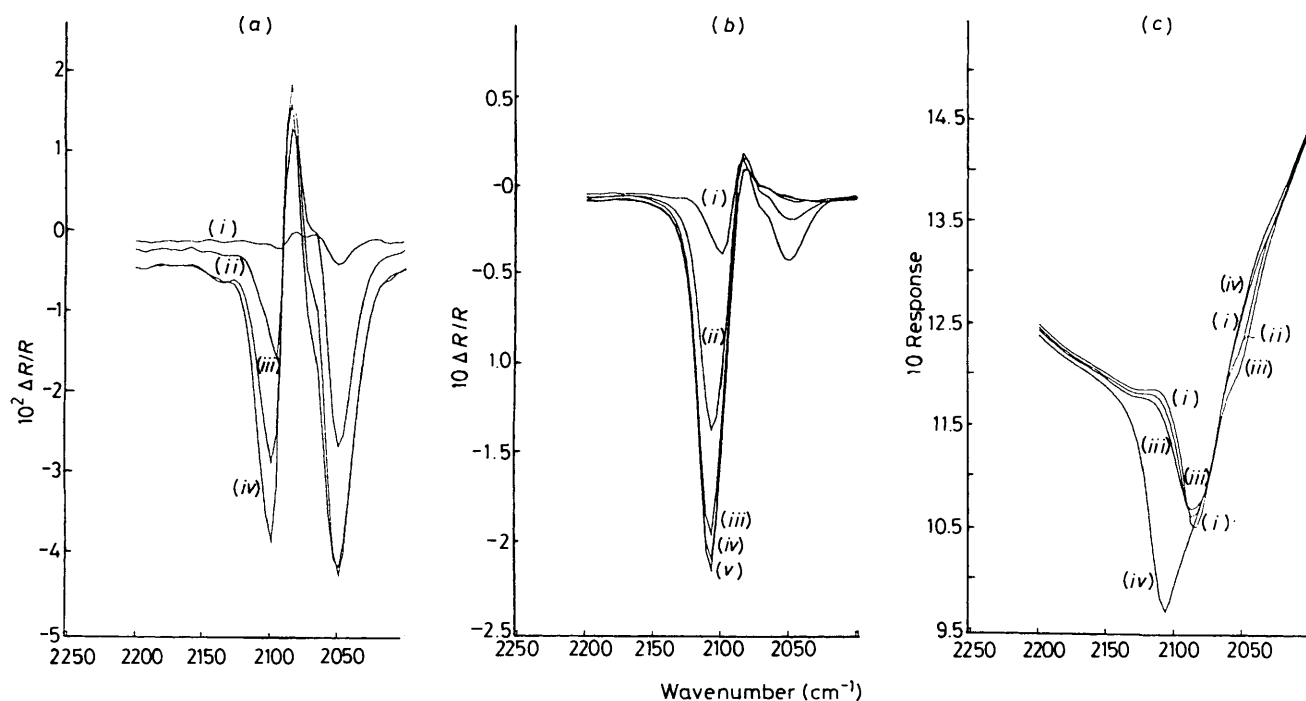
Figure 2. (a) and (b) Subtractively normalised F.t.i.r. spectra (resolution 8 cm^{-1}, 69 scans) of a film grown and cycled in a manner exactly analogous to that of Figure 1, collected using 0.5 mol dm^{-3} KCl electrolyte. The reference (s.b.) spectrum was collected at the base potential of -0.3 V. Further s.b. spectra were then collected at successively higher potentials and normalised to the reference spectrum to give the data shown in the Figures. E/V: -0.2 (i), 0 (ii), 0.1 (iii), and 0.15 (iv); (b) 0.15 (i), 0.2 (ii), 0.3 (iii), 0.4 (iv), and 0.5 (v). (c) Representative s.b. spectra from the experiments in 2(a) and (b). E/V: 0.3 (i), 0 (ii), 0.1 (iii), and 0.5 (iv)
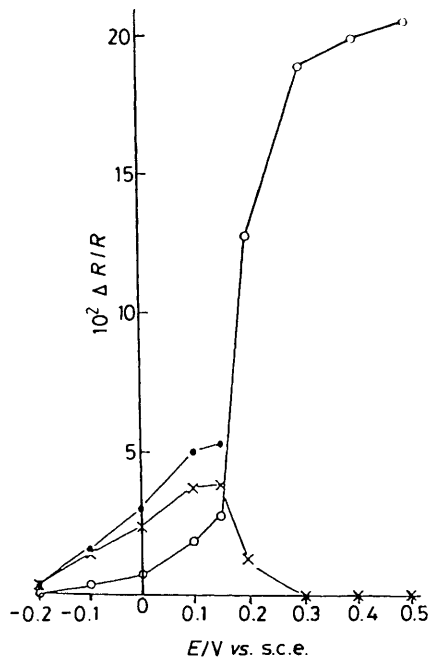

Figure 3. Plots of the intensities of the bands observed in Figure 2 vs. potential (○) 2 100-cm^{-1} gain feature, (×) 2 050-cm^{-1} gain feature, and (●) 2 080-cm^{-1} loss feature. The latter feature cannot be distinguished beyond 0.15 V

together with a transitory peak at 2 050 cm^{-1}. On further reduction and reoxidation, the peak at 2 106 cm^{-1} continues to grow, eventually dominating the spectrum of PB, whereas the peak at 2 075 cm^{-1} declines to a poorly resolved shoulder.

In order to understand the processes taking place, the nature of the Prussian Blue film must be explored in more detail.

Unless the films are grown very slowly and carefully, they usually show poorly resolved X-ray diffraction patterns,[17] suggesting that the structure is relatively amorphous. Our ellipsometric measurements[13] identified an inner relatively compact layer and an outer, more porous region, and the process of oxidation was found to involve first the conversion of the outer porous layer and then the more rapid and reversible conversion of the inner compact layer by an interesting mechanism in which layers of PB and PW coexist, with the boundary between the two moving steadily into the film from the outer edge.

The lack of structure in the X-ray diffraction data suggests that local ordering may only extend over a few nm. Therefore, the structure of the film is either that of a 'glassy' material, consisting of relatively random co-ordination about the iron centres, or a 'particle hydrate' in which small (<5 nm) particles of PB are held together by hydrogen bonding or, possibly, cyanide bridges.[18] The substantial water content revealed by electrochemical quartz-crystal microbalance data,[10] even for the inner layer, suggests the aqueous particle hydrate model may be the more reasonable. Ellipsometric data suggest that the outer layer contains additional water and, possibly, smaller particles.

With this model in mind, we first consider the behaviour of the film during the early cycling process. As indicated above, PB is believed to be deposited as the 'insoluble' form whose structure is now known to be appreciably different from the classical Keggin–Miles model.[6] With reference to Figure 5, which shows a unit cell of the 'PB structure,' the 'insoluble' form has vacancies on $\frac{1}{4}$ of the 24e and 4b sites of the $Fm3m$ parent lattice {which correspond to the 6e,6f,12h and 1b,3d sites of the most likely $Pm3m$ structure of $Fe_4[Fe(CN)_6]_3\cdot14H_2O$ phase}.[7] Water is present not only in the zeolitic-type 8c sites (8g of $Pm3m$) but in the $\frac{1}{4}$ vacancies on the 24e sites. Thus, on average, each high-spin Fe^{3+} ion has two oxygen and four nitrogen neighbours. In fact, it is likely that these Fe^{3+} ions will be
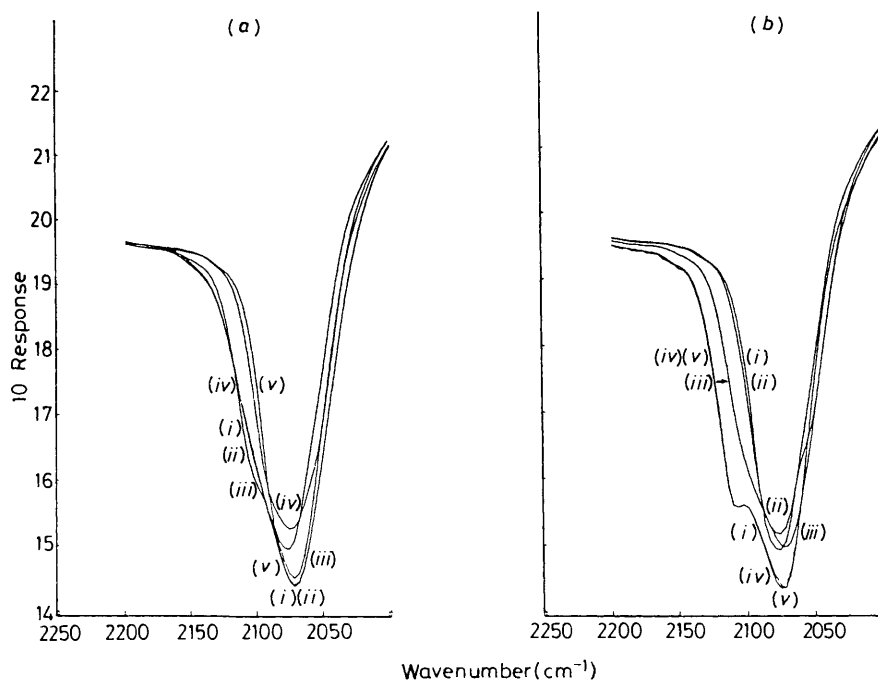
(a)

(b)

Wavenumber(cm⁻¹)

Figure 4. Single-beam spectra of a Prussian Blue film grown for 60 s as described in the text. At the end of this period the potential was maintained at + 0.5 V and the electrolyte was replaced with 0.1 mol dm⁻³ KCl. Spectra were then collected at 0.5 V and successively lower potentials [the cathodic sweep, Figure 4(a)] down to − 0.2 V. The potential was then stepped up to + 0.5 V again and spectra collected during the anodic sweep [Figure 4(b)]. E/V: (a) 0.5 (i), 0.4 (ii), 0.2 (iii), 0 (iv), and −0.2 (v); (b) −0.2 (i), 0 (ii), 0.2 (iii), 0.4 (iv), and 0.5 (v)
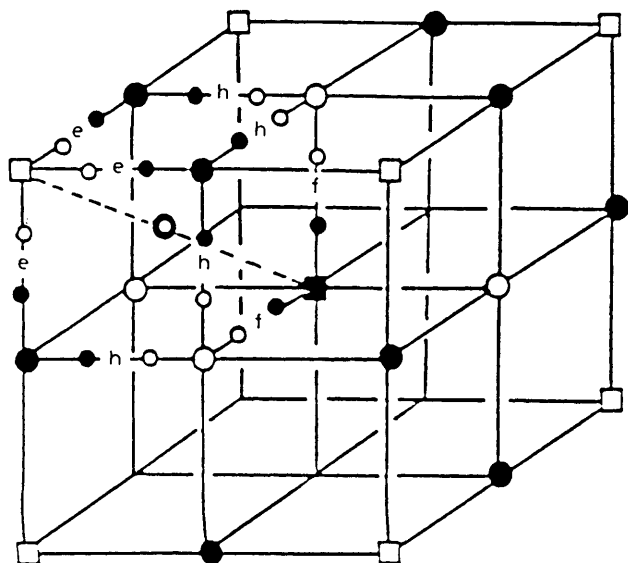

Figure 5. The unit cell of Prussian Blue in space group $Pm3m$. The atom types of crystallographic positions are partially indicated by the following symbols: □, Fe^{III}, 1a (origin); ○, Fe^{III}, 3c; ■, Fe^{II}, 1b; ●, Fe^{II}, 3d; ○, O, 8g; ●, C, 6e, 6f, 12h; ○, N or O, 6e, 6f, 12h. Redrawn from Figure 1 of ref. 7(a)

hydrolysed and present as $[Fe(OH)]^{2+}$, as suggested by Lundgren and Murray.[11b] By contrast, the structure of 'soluble' PB is believed to be $Fm3m$ type with all 4b and 24e sites occupied, with charge neutralisation through K^+ ions on half the 8c sites.

Reduction of the initial film of 'insoluble' PB must involve the gradual incorporation of K^+ ions into the 8c sites, but the i.r. spectra reveal that the process is quite complex. Assuming that the final spectra of Figure 2 in the PB region are dominated by the 'soluble' form, we can assign the band at 2 106 cm⁻¹ to a

$Fe^{II}-C≡N \cdots Fe^{3+}$ bridge; from the spectrum of PW we can similarly assign the peak at 2 080 cm⁻¹ to a $Fe^{II}-C≡N \cdots Fe^{2+}$ bridge [where Fe^{II} and Fe^{2+} refer respectively to low- and high-spin iron(II) ion]. Given that the v_6 band of $[Fe(CN)_6]^{4-}$ in solution is found at 2 044 cm⁻¹ and in $K_4[Fe(CN)_6]·3H_2O$ at 2 033 cm⁻¹ (ref. 1), we may tentatively associate a ca. 20 cm⁻¹ shift in the CN stretching frequency for every unit positive charge increase in the cation to which the N is co-ordinated. The broad spectrum for the insoluble form, with a maximum near 2 075 cm⁻¹, must then be associated with a $Fe^{II}-C≡N \cdots Fe(OH)^{2+}$ unit, or something similar.

A problem with this mechanism is that the material initially formed on reduction will have the formulation $K_4(Fe^{2+})_4[Fe^{II}(CN)_6]_3[H_2O\{24e\}]_x$. The steady loss of H_2O from the 24e sites and the shift in $v(CN)$ both point to eventual formation of $K_2Fe^{2+}[Fe^{II}(CN)_6]$ as the final form of PW. It is likely that PW crystallites are simply not stable with vacancies on the $Fe^{II}(CN)_6$ sites, a suggestion supported by the known crystal structure of $Cs_2Mg[Fe(CN)_6]$,[19] which has a true Keggin structure with no water on the 24e sites, or indeed on the zeolitic 8c sites. The conversion of the initially formed material to the final form of PW involves some loss of Fe^{2+} from the lattice and its eventual removal from the film and replacement with K^+. Since K^+ only occupies the 8c sites, the lattice must, in effect, close up. That it is able to do so without significant film degradation is a further indication that a particle hydrate model is the best description of the film structure, with extensive water of solvation about each small crystallite of PW. The extrusion of Fe^{2+} from the 4a sites and concomitant loss of vacancies on the $Fe^{II}(CN)_4$ 4b sites cannot be a simple process, and the i.r. data suggest that several potential cycles, at least in the films prepared by ourselves, may be necessary before the film is substantially converted.

There remains the problem of the small transitory peaks seen on the first reduction cycle at 2 106 cm⁻¹ and on subsequent cycles near 2 050 cm⁻¹. The high-frequency peak is straightforward: almost certainly the dynamic reduction process of
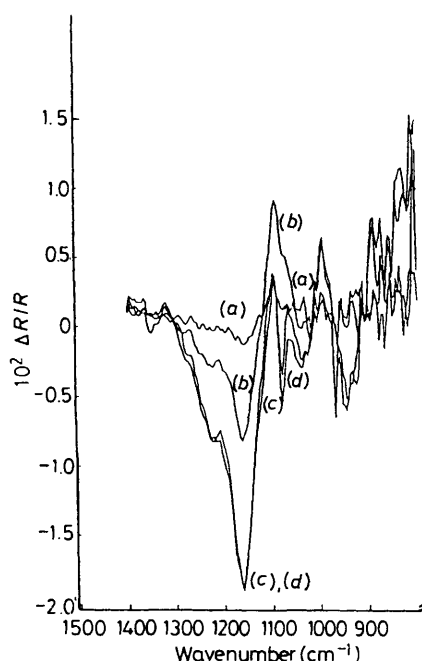
Figure 6. Difference spectra for a Prussian Blue film grown for 30 s as described above and cycled in 0.1 mol dm^{-3} KH$_2$PO$_4$–K$_2$HPO$_4$–0.1 mol dm^{-3} KCl buffer at pH 6. Spectra were collected at successively higher potentials and normalised to the reference spectrum taken at -0.3 V. E/V: -0.2 (a), 0 (b), 0.2 (c), and 0.5 (d). The gain features at 1 221 (sh), 1 160, and 1 078 cm^{-1} are assigned to H$_2$PO$_4^-$ and the loss features at 1 088 and 990 cm^{-1} are due to HPO$_4^{2-}$

insoluble PB will be accompanied *initially* by migration of protons in the film, since H$^+$ has a much higher mobility and its incorporation is favoured by the structure of the insoluble form. Reduction of the pH in the film will lower the extent to which the Fe^{3+} is hydrolysed in the insoluble PB material and some true Fe^{II}–C≡N $\cdots$ Fe^{3+} bridges form. As the cycle progresses, Fe^{3+} is reduced to Fe^{2+} throughout the structure, and Fe^{II}–C≡N $\cdots$ Fe^{2+} bridges form. The persistence of the peak at 2 106 cm^{-1} on initial reoxidation of the Prussian White film first formed suggests that even after the first cycle an appreciable conversion into the *soluble* form has taken place, with some Fe^{3+} ions now surrounded by six NC groups. For the remaining 'insoluble' PW, which still has H$_2$O on the 24e sites, it is probable that the reoxidation to insoluble PB is accompanied by a reversal of the initial reduction process. In this case, H$^+$ is first expelled and the pH inside the film rises, causing hydrolysis of the Fe^{2+} ions to [Fe(OH)]$^+$. This will lower ν(CN) to *ca.* 2 060 cm^{-1} if we use the shift of 20 cm^{-1} per unit change in positive charge described above. Oxidation of {Fe(OH)}$^+$ to [Fe(OH)]$^{2+}$ then takes place to yield the insoluble PB. Note that this mechanism requires that there is some residual insoluble PB remaining in the film, which is certainly consistent with the persistent shoulder near 2 075 cm^{-1} in the s.b. spectra of well cycled PB.

Reduction of insoluble PB should be accompanied by marked changes in the O–H stretching region as the Fe^{2+} formed on reduction is unlikely to be so extensively hydrolysed; such changes are indeed observed, with the loss of structure near 2 800 cm^{-1} being particularly marked in earlier cycles. These changes in the O–H region are greatly diminished in later cycles on the same film; apparently the H$_2$O on the 24e sites disappears as the main ν(CN) band moves to 2 106 cm^{-1}.

In addition, if our model is correct, we would expect to observe a pH change in the electrolyte in the immediate vicinity of the electrode during the oxidation of insoluble PW to PB.

This is detectable in the subtractively normalised F.t.i.r. experiment; the i.r. beam samples the thin layer of electrolyte between the working electrode and cell window, in addition to the film. By employing a phosphate buffer, changes in the intensity of bands due to HPO$_4^{2-}$ and H$_2$PO$_4^-$ can be monitored.[15] The results of such an experiment are shown in Figure 6 for the reoxidation of a well cycled film. As can be seen, loss features appear at 1 070, 1 055, and 993 cm^{-1}, corresponding to HPO$_4^{2-}$, and gain features are observed at 1 230 (sh), 1 160, 1 072, and 947 cm^{-1} due to H$_2$PO$_4^-$. The positions of these features are in good agreement with those given in the literature.[20] The spectra in Figure 6 are somewhat confused in the region between 1 100 and 900 cm^{-1} owing to the fact that both H$_2$PO$_4^-$ and HPO$_4^{2-}$ have overlapping features here; the resultant spectra show, therefore, rather complex profiles. What Figure 6 does show very clearly is that the pH in the thin layer has dropped owing to the expulsion of protons from the film. This is in agreement with our model: the film expels protons as the residual insoluble PB reforms, but no further change occurs as the soluble PB forms.

If we now put together what we have learned from ellipsometry and i.r. spectroscopy we reach the following conclusions: the film is initially insoluble PB, which grows as a relatively compact inner layer and, at higher thicknesses, also forms an outer more porous layer. The bulk of the film is converted into soluble PB on potential cycling, but some of the outer porous film remains in the insoluble form. The relative amounts of the soluble and insoluble forms are likely to depend very sensitively on the manner in which the film is grown, and i.r. spectroscopy reveals the presence of both forms of the film very clearly.

We can also establish a tentative connection between the cyclic voltammogram and the spectroscopic data. It will be seen from Figure 1 that there are broad oxidation and reduction features between -0.2 and $+0.15$ V, precisely in the region where the transient features appear in the i.r. spectra. On the basis of the analysis above, these features must be associated with redox cycling of the *insoluble* form, and the sharp feature near $+0.18$ V can then be assigned to oxidation of the *soluble* form. This is supported by ellipsometric data,[13] that showed a major change in the inner, compact film taking place at this potential, and found changes in the outer film occurring over a much wider potential range corresponding to the broad features in the cyclic voltammogram.

(*c*) *Interconversion of Prussian Blue and Prussian Yellow.*— The oxidation of PB is far less reversible in our films than the reduction and the cyclic voltammogram shows an indeterminate anodic wave starting at 0.8 V with a peak near 0.95 V.[13] A reverse peak, at 0.85 V, can be seen on the reverse sweep. The difference spectra are of much less help here than the s.b. spectra; the former are shown in Figure 7(*a*) with the s.b. spectra, referred to a reference spectrum at 0.5 V, in Figure 7(*b*). It should be noted that these spectra were obtained for a film that had been well cycled and therefore contained mainly soluble PB. It is clear that there is a marked reduction in the peak associated with soluble PB, at 2 106 cm^{-1}, and the appearance of a residual peak near 2 080 cm^{-1} together with a peak at *ca.* 2 175 cm^{-1}. Of the latter there can be little doubt that it is the peak corresponding to a Fe^{III}–CN $\cdots$ Fe^{III} bridge. The position of the [Fe^{III}(CN)$_6$]$^{3-}$ ν_6 cyanide stretch is at 2 118 cm^{-1} in solution and at 2 115 cm^{-1} in the solid. Adding 60 cm^{-1} as the estimated shift for the terminal Fe^{3+} gives us *ca.* 2 175 cm^{-1}, essentially identical to that observed. This then is the peak corresponding to cyanide in the Keggin structure of PY, from which all K$^+$ ions have been expelled and, presumably, replaced with water.

The peak at *ca.* 2 080 cm^{-1} can only be due to cyanide co-ordinated to Fe^{II}, since even unco-ordinated [Fe^{III}(CN)$_6$]$^{3-}$ lies
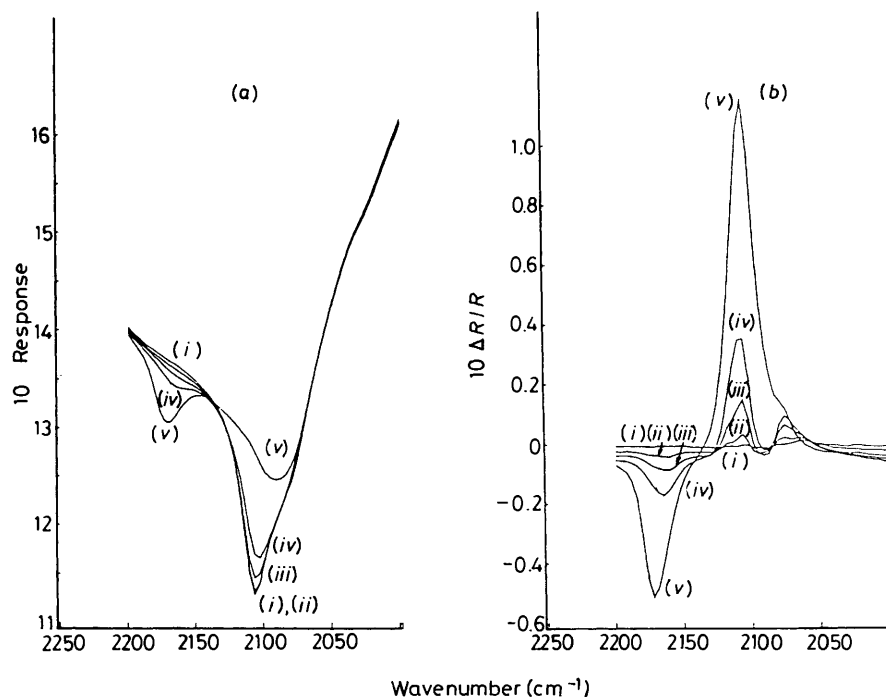
Wavenumber (cm⁻¹)

Figure 7. (a) Single-beam spectra of a Prussian Blue film grown and cycled in the same manner as that in Figure 1. The spectra were collected at +0.5 V and successively higher potentials (V): 0.6 (i), 0.7 (ii), 0.75 (iii), 0.8 (iv), and 0.9 (v). (b) The spectra in (a) normalised to the first collected at 0.5 V (i.e. subtractively normalised F.t.i.r. spectra, base potential +0.5 V)

above 2 100 cm⁻¹, and cation co-ordination must raise v(CN). It is also unlikely that it represents any formally forbidden i.r. band such as the A_{1g} or E_g vibrations of the octahedral $[Fe^{III}(CN)_6]^{3-}$ complex that have become allowed by loss of symmetry, since the band is exceedingly intense; in any case, Raman data place these two bands *higher* in frequency for $[Fe^{III}(CN)_6]^{3-}$ than the allowed T_{1u} band. The proximity of the band at 2 080 cm⁻¹ to that associated with insoluble PB give us an important clue as to its assignment. The cyclic voltammogram indicates incomplete conversion of PB into PY at the potentials accessed, and ellipsometry also suggests that the outer porous layer is sluggish in conversion. Taken together, we assign the band at 2 080 to unconverted insoluble PB. It would appear that insoluble PB cannot be converted into PY with any facility, a conclusion hardly surprising in view of the fact that the only cation that could be expelled from the lattice is H⁺, whose loss would lead to to hydrolysis of Fe³⁺ on a substantial scale and the precipitation of Fe(OH)₃ from the film. Of course, conversion might also be effected by incorporation of anions, but this also appears to be a slow process, since most anions are too large to fit into the zeolitic 8c sites, and incorporation of anions only into the inter-particle space will lead to large charges building up on the particles.

References

1 A. G. Sharpe, 'The Chemistry of Cyano Complexes of the Transition Metals,' Academic Press, London, 1976.
2 K. Itaya, I. Uchida, and V. D. Neff, *Acc. Chem. Res.*, 1982, 19, 162.
3 R. J. Mortimer and D. R. Rosseinsky, *J. Electroanal. Chem.*, 1983, 151, 133.
4 D. W. DeBerry and Z. Viehbeck, *J. Electrochem. Soc.*, 1983, 130, 249.
5 V. D. Neff, *J. Electrochem. Soc.*, 1985, 132, 1382.
6 J. F. Keggin and F. D. Miles *Nature (London)*, 1936, 137, 577.
7 (a) H. J. Buser, D. Schwarzenback, W. Petter, and A. Ludi, *Inorg. Chem.*, 1977, 16, 2704; (b) R. J. Mortimer and D. R. Rosseinsky, *J. Chem. Soc., Dalton Trans.*, 1984, 2059.
8 V. D. Neff, *J. Electrochem. Soc.*, 1978, 125, 886.
9 K. Itaya and I. Uchida, *Inorg. Chem.*, 1986, 25, 389; K. Itaya, T. Ataka, and S. Toshima, *J. Am. Chem. Soc.*, 1982, 104, 4767.
10 B. J. Feldman and O. R. Melroy, *J. Electroanal. Chem.*, 1987, 234, 213.
11 (a) B. J. Feldman and R. W. Murray, *Inorg. Chem.*, 1987, 26, 1702; (b) C. A. Lundgren and R. W. Murray, *ibid.*, 1988, 27, 933.
12 P. A. Christensen, J. C. H. Kerr, S. J. Higgins, and A. Hamnett, *Faraday Discuss. Chem. Soc.*, 1989, 88, 261.
13 A. Hamnett, S. J. Higgins, R. J. Mortimer, and D. R. Rosseinsky, *J. Electroanal. Chem.*, 1988, 255, 315.
14 A. Bewick and S. Pons, *Adv. Infra-red Raman Spectrosc.*, 1985, 12, 1.
15 P. A. Christensen and A. Hamnett, *Comp. Chem. Kinetics*, 1989, 29, 1.
16 P. A. Christensen, A. Hamnett, and P. R. Trevellick, *J. Electroanal. Chem.*, 1988, 242, 23.
17 T. Ikeshoji and T. Iwasaki, *Inorg. Chem.*, 1988, 27, 1123.
18 W. A. England, M. G. Cross, A. Hamnett, P. J. Wiseman, and J. B. Goodenough, *Solid State Ionics*, 1980, 1, 231.
19 B. I. Swanson, S. I. Hamburg, and R. R. Ryan, *Inorg. Chem.*, 1974, 13, 1685.
20 A. C. Chapman and L. E. Thirlwell, *Spectrochim. Acta*, 1964, 20, 937.